Interference of a Mutant Thyroid Hormone Receptor α1 with Hepatic Glucose Metabolism

Milica Vujovic, Kristina Nordström, Karine Gauthier, Frédéric Flamant, Theo J. Visser, Björn Vennström, and Jens Mittag

Karolinska Institutet (M.V., K.N., B.V., J.M.), Department of Cell and Molecular Biology, 17177 Stockholm, Sweden; Institut de Génomique Fonctionnelle de Lyon (K.G., F.F.), Université de Lyon, Université Lyon 1, Centre National de la Recherche Scientifique, Institut National de la Recherche Agonomique, Ecole Normale Supérieure de Lyon, 69007 Lyon, France; and Erasmus Medical Center (T.J.V.), Department of Internal Medicine, 3000 DR Rotterdam, The Netherlands

Downloaded from https://academic.oup.com/endo/article/150/6/2940/2456385 by guest on 21 August 2022

Mice expressing the mutant thyroid hormone receptor TRα1R384C, which has a 10-fold reduced affinity to the ligand T_3, exhibit hypermetabolism due to an overactivation of the sympathetic nervous system. To define the consequences in the liver, we analyzed hepatic metabolism and the regulation of liver genes in the mutant mice. Our results showed that hepatic phosphoenolpyruvate-carboxykinase was up-regulated and pyruvate kinase mRNA down-regulated, contrary to what observed after T_3 treatment. In contrast, mice expressing a mutant TRα1L400R specifically in the liver did not show a dysregulation of these genes; however, when the TRα1L400R was expressed ubiquitously, the hepatic phenotype differed from TRα1R384C animals, suggesting that the localization of the mutation plays an important role for its consequences on glucose metabolism. Furthermore, we observed that glycogen stores were completely depleted in TRα1R384C animals, despite increased gluconeogenesis and decreased glycolysis. Exposure of the mutant mice to high maternal levels of thyroid hormone during fetal development leads to a normal liver phenotype in the adult. Our results show how genetic and maternal factors interact to determine the metabolic setpoint of the offspring and indicate an important role for maternal thyroid hormone in the susceptibility to metabolic disorders in adulthood. **(*Endocrinology* 150: 2940–2947, 2009)**

Thyroid hormone (TH) is essential for normal tissue development, differentiation, and energy homeostasis in mammals. It controls a wide variety of regulatory events in metabolic pathways, which determine overall energy expenditure and basal metabolic rate (1). The pleiotropic actions of TH are mediated by the nuclear TH receptor (TR) α1 and TRβ, which are encoded by separate genetic loci (2). TRs bind to TH-responsive elements in DNA and stimulate the expression of positively regulated target genes in the presence of the ligand as holoreceptors, although repressing it in the absence of ligand as aporeceptors. This regulatory mechanism applies in an opposite manner to negatively regulated TH target genes.

TRs exert overlapping but also isoform-specific functions. TRα1 is most relevant for proper brain development (3–5), whereas TRβ plays a major role in the regulation of liver genes (6), representing more than 85% of T_3-binding activity in this tissue (7). Mutations in TRβ are the underlying cause of the human syndrome resistance to TH (8). Surprisingly, no patients have been identified harboring a germline mutation in TRα1. To understand the consequences of such a defect and to define the physiological role of apo-TRα1, mice heterozygous for the TRα1R384C mutation (TRα1+m mice) were generated (9). The mutant TRα1 has a 10-fold lower affinity to TH, thus acting as an aporeceptor under physiological TH concentrations. Besides a prominent neurological phenotype including high anxiety and locomotor deficiencies (5, 10), the mice have normal TH levels as adults but exhibit a strong hypermetabolism (11). As consequence, the animals are lean despite being hyperphagic and resistant to diet-induced obesity, and their fat depots are reduced. However, they maintain euglycemia and do not require additional ketogenesis to maintain energy homeostasis. Most interestingly, this phenotype resembles hyper- rather than hypothy-

ISSN Print 0013-7227 ISSN Online 1945-7170
Printed in U.S.A.
Copyright © 2009 by The Endocrine Society
doi: 10.1210/en.2008-1085 Received July 21, 2008. Accepted February 27, 2009.
First Published Online March 12, 2009

Abbreviations: Acyl-CoA-DH, Acyl-coenzyme A dehydrogenase; BAT, brown adipose tissue; DTT, dithiothreitol; E10.5, embryonic d 10.5; FAS, fatty acid synthetase; nt, nucleotide; P15, postnatal d 15; PEPCK, phosphoenolpyruvate carboxykinase; PK, pyruvate kinase; qPCR, quantitative PCR; TH, thyroid hormone; TR, TH receptor.

roidism, which would be the expected outcome of an apo-TRα1. The apparent discrepancy is explained by a novel central action of apo-TRα1 that causes a high sympathetic output leading to a hypermetabolic brown adipose tissue (BAT). The hypothesis is supported by the fact that the hypermetabolism is reversed if the animals are housed at thermoneutrality where BAT gets functionally denervated (11).

The centrally induced hypermetabolism of the BAT at room temperature has secondary effects on other tissues such as the liver, the key player in glucose homeostasis. Because it is well known that TRα1 also interferes directly with enzymes involved in hepatic glucose metabolism (12, 13), TRα1+m mice are a valuable animal model to study the interactions of hypermetabolism and impaired TRα1 signaling in the liver.

Here we show that TRα1+m mice respond to the hypermetabolism by increasing hepatic gluconeogenesis and decreasing glycolysis. In addition, the expression of the rate-limiting enzymes is directly and region-specifically affected by the mutant TRα1, opposite to what is expected from T_3-treated wild-type animals. Moreover, glycogen stores are completely depleted in the TRα1+m mice. These deficiencies are not observed when the mutants are exposed to high maternal levels of TH during fetal development, demonstrating that genetic and maternal factors interact to determine the metabolic setpoint of the offspring.

Materials and Methods

Experimental animals

The mouse strain carrying the dominant-negative R384C mutation in TRα1 and the combination with a TRβ-null allele have been described previously (5, 9). The TRα1R384C mice used for the experiments have been backcrossed to C57BL6/6NCrl for eight to 10 generations. If not indicated otherwise, heterozygous male mutants and wild-type littermates were born by wild-type females, and five animals per group were used for the experiments at the age of 4–7 months. The animals were housed at 21 C on a 12-h light, 12-h dark cycle. For thermoneutrality studies, mice were transferred to 30 C at the age of 2 months and kept at this temperature for 6 wk. T_3 treatment was performed for 12 d via drinking water containing 0.01% albumin and 0.5 μg/ml T_3. Blood glucose levels were determined using the AccuCheck Sensor glucose detection system (Roche, Mannheim, Germany). For hepatic cultures, livers were extracted, cut into pieces, washed twice with warm PBS, and then incubated at 37 C for 6 h in DMEM (Invitrogen, Uppsala, Sweden) containing 0.1% glucose, 10% stripped fetal calf serum, and 10 nM T_3. Animal care procedures were in accordance with the guidelines set by the European Community Council Directives (86/609/EEC). Required ethical permissions were obtained from the local ethical committees.

TH levels in the animal models

Serum and tissue TH levels of the different animal models including the combinations with TRβ inactivation have been analyzed in detail previously (5, 9, 10). Briefly summarized, adult TRα1+m mice did not display significant difference in serum T_3 and T_4 levels compared with wild-type animals. After the oral T_3 treatment, hepatic T_3 levels were 10-fold elevated, thus reactivating the mutant TRα1 (10). The inactivation of TRβ in TRα1+m animals caused a 10-fold elevated T_4 level in the serum compared with wild-type (5, 9). These animals have been used as mothers to expose the offspring to high maternal levels of TH during pregnancy. Exposure to high levels of maternal TH had no effect on the T_4 serum levels in the offspring TRα1+m mutant mice (5).

Mice with a hepatic mutant TRα1

Mice expressing the TRα1L400R mutation in hepatocytes from the fetal stage were produced by crossing heterozygous AFLP-Cre mice (14) with TRαAMI/TRαAMI homozygous mice. These mice carry a THRA knock-in allele in which the deletion of a floxed cassette enables the expression of a cDNA carrying the TRα1L400R reading frame (15). Littermates that did not inherit the CRE gene were used as controls.

In situ hybridization

Digoxigenin-labeled RNA probes were generated from cDNA subclones in pGEM-T easy plasmids (Promega, Mannheim, Germany). *In vitro* transcription was carried out according to standard protocols using a DIG RNA Labeling Kit (Roche). Probes were generated from cDNA fragments corresponding to nucleotides (nt) 40-1055 of deiodinase type I (accession no. NM_007860), nt 896-1296 of phosphoenolpyruvate carboxykinase (PEPCK accession no. NM_011044), nt 1066-1478 of pyruvate kinase (PK; accession no. BC152327), nt 5789-6189 of fatty acid synthetase (FAS; accession no. BC046513), nt 236-633 of acyl-coenzyme A dehydrogenase (Acyl-CoA; accession no. NM_007381), and nt 1494-1797 of E-cadherin (accession no. NM_009864). cRNA probes were diluted in hybridization buffer [50% formamide, 10% dextran sulfate, 0.05% tRNA, 0.6 M NaCl, 10 mM Tris·HCl (pH 7.4), 1× Denhardt's solution, 100 μg/ml sonicated salmon sperm DNA, 1 mM EDTA, and 10 mM dithiothreitol (DTT)] to a final concentration of 10 ng/μl.

After the animals were decapitated, livers were removed rapidly, embedded in Tissue-Tek medium (Sakura Finetek, Torrance, CA), and frozen on dry ice. Sections of 20 μm were cut on a cryostat, thaw-mounted on silane-treated slides, and stored at −80 C until further processing. *In situ* hybridization was carried out as described previously (16). Representative fields of 1 × 1.5 mm from cross-sections were chosen and documented with a Nikon Eclipse 50 microscope. For quantification, the *in situ* hybridization was performed with radioactive probes labeled with [^{35}S]UTP (25,000 cpm/μl; Hartmann Analytik, Braunschweig, Germany), which were visualized on a Biomax MR x-ray film (Kodak, Sigma Aldrich, Taufkirchen, Germany). Signals were quantified using NIH ImageJ software. For colocalization, [^{35}S]UTP-labeled radioactive probes (50,000 cpm/μl; Hartmann Analytik) for E-cadherin were generated and mixed with digoxigenin-labeled probes of PEPCK (20 ng/μl). After visualization of PEPCK transcripts as described above, the sections were dehydrated and exposed to Biomax MR x-ray films (Kodak, Sigma Aldrich), and corresponding areas on the film and the section were documented. Sense probes that were used to confirm the specificity of the hybridization reaction did not show any signal (data not shown).

Real-time PCR

RNA was isolated from snap-frozen tissues using the RNeasy Mini Kit (QIAGEN, Uppsala, Sweden) according to the manufacturer's instructions. cDNA was generated using reverse transcription with Oligo-dT primers and used for real-time PCR with the ABI 7300 system and the ABI Prism 7000 (Applied Biosystems, Stockholm, Sweden). A standard curve was used to correct for PCR efficiency, and the results were normalized using HPRT as reference gene. The quantification was done over 40 cycles, but all calculated threshold cycles were less than 30. An additional melting curve was recorded to confirm the specificity of the reaction. Primer sequences are available on request.

D1 activity

Liver tissue was homogenized in 10 vol 0.1 M phosphate (pH 7.2), 2 mM EDTA (PE buffer) containing 1 mM DTT. For measurement of D1 activity, about 2 μg homogenate protein was incubated for 30 min at 37 C with 0.1 μM (2 × 10^5 cpm) [3′,5′-^{125}I]rT_3 in a final volume of 100 μl PE buffer containing 10 mM DTT. The reactions were stopped by addition of 100 μl ice-cold ethanol, and the mixtures were processed and

Downloaded from https://academic.oup.com/endo/article/150/6/2940/2456385 by guest on 21 August 2022

analyzed for production of [^{125}I]- and [3,3′-^{125}I]T_2 by HPLC as previously described (17).

Enzyme activity and glycogen content determination

Snap-frozen tissue was homogenized in 4 vol of a potassium phosphate buffer (pH 7.0) containing 1 mM DTT. Cytosolic fractions of three to five animals per group were obtained by centrifugation for 1 h at 100,000 × *g* and tested for PEPCK activity in a sample buffer containing 65 mM Tris (pH 8.0), 6 mM $MgCl_2$, 15 μM $MnCl_2$, 0.875 mg/ml BSA, 4.65 mM ATP and ADP, 0.6 mM reduced nicotinamide adenine dinucleotide, and 5 U/ml PK and lactate dehydrogenase. Oxaloacetate was added as substrate in a final concentration of 0.5 mM, and the conversion of reduced nicotinamide adenine dinucleotide was monitored at 340 nm. Samples without substrate and samples with water were used to determine background activity. Activities were normalized against the protein content of the sample. For PK activity, the same cytosolic fractions and sample buffer were used, except without $MnCl_2$, ATP, and PK, and 0.5 mM phosphoenolpyruvate was used as substrate.

Glycogen content in the liver was determined as described (18) with minor modifications. Briefly, 10–20 mg snap-frozen liver tissue of five animals per group were homogenized in 1 ml 5% trichloroacetic acid and incubated for 30 min at room temperature. After centrifugation at 20,000 × *g* for 10 min, glycogen was precipitated from the supernatant by adding 2 vol of 95% ethanol and centrifugation at 20,000 × *g* for 30 min. The supernatant was discarded and the precipitate dissolved in a 1:60 dilution of Lugol's reagent (Sigma-Aldrich) in 25% (wt/vol) potassium chloride containing 30 mM hydrochloric acid. The glycogen content was determined spectrophotometrically at 600 nm and normalized against the tissue weight.

Statistical analyses

If not stated otherwise, the values represent mean ± SEM. Statistical comparisons of real-time PCR data were done using two-way ANOVA to compare the effects of TH treatment on both genotypes (supplemental Fig. 1A, published as supplemental data on The Endocrine Society's Journals Online web site at http://endo.endojournals.org). If required, single groups were subsequently compared using Student's *t* test. In all other experiments a two-tailed Student's *t* test was applied, and significant changes have been marked accordingly in the figures.

Results

Expression of TH target genes in livers of TRα1+m mice

To identify impairments caused by the mutant TRα1, we analyzed the expression of known TH target genes in the liver by quantitative PCR (qPCR) (Fig. 1A and supplemental Fig. 1A). The expression of spot14 was found to be equal in the two genotypes and similarly up-regulated by T_3. Although the qPCR showed a small, albeit not significant, up-regulation of deiodinase type I transcript levels in the mutant mice, this increase was more obvious in the corresponding *in situ* hybridization (Fig. 1B) and in deiodinase type I activity assays in liver homogenates (Fig. 1C and statistics in supplemental Fig. 1A). However, upon T_3 treatment, the mRNA levels in qPCR and *in situ* hybridization as well as the enzymatic activities were significantly increased to a similar level in wild-type and TRα1+m animals.

We then analyzed the mRNA level of β-catenin, an important factor in liver development and zonation (19) and a direct target of TRα1 in the intestine (20). The expression of this gene was not altered in the mutant mice and did not significantly change upon T_3 treatment. Similar results were obtained for the TH transporter MCT8, which was in agreement with previous observations in the brain (21). Taken together, apo-TRα1 seems to play only a minor role in D1 mRNA regulation, but no major effect was observed for the regulation of the other genes analyzed.

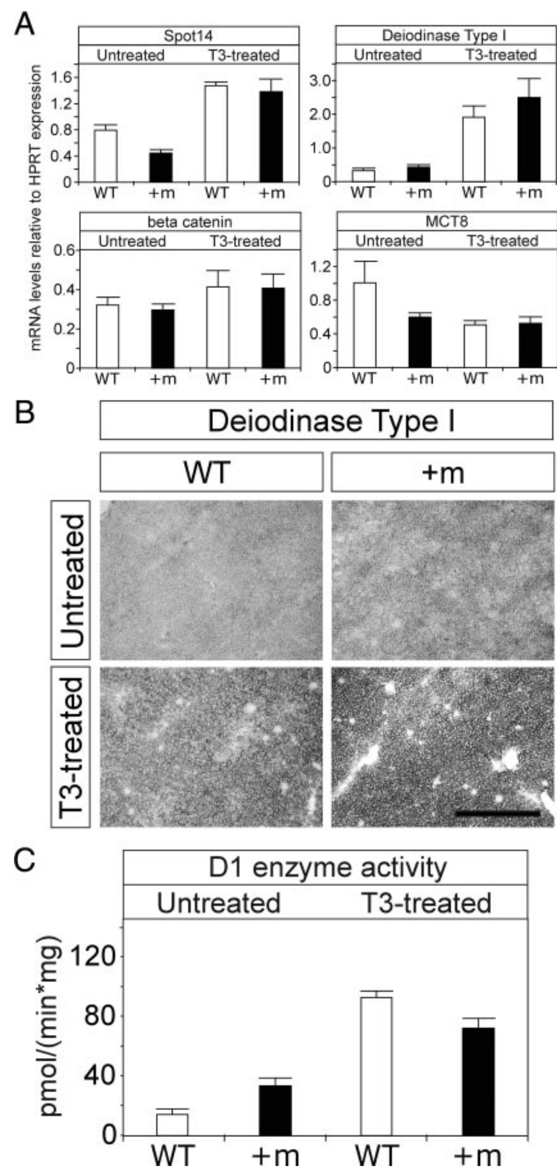

FIG. 1. A, mRNA expression levels of potential TH target genes in livers of untreated and T_3-treated wild-type (WT) and mutant (+m) animals, as analyzed by qPCR and normalized against HPRT as reference gene; B, *in situ* hybridization histochemistry showing the expression of deiodinase type I mRNA in liver sections of untreated and T_3-treated wild-type (WT) and mutant animals (+m); C, enzyme activity of deiodinase type I (D1) in liver homogenates of untreated and T_3-treated wild-type (WT) and mutant animals (+m). *Scale bar* in B, 500 μm.

Expression of metabolic genes in livers of TRα1+m mice

Mice with a dominant-negative TRα1 exhibit hypermetabolism at room temperature (11). To characterize the consequences for liver metabolism, we performed *in situ* hybridization with marker genes for fatty acid degradation (acyl-CoA-DH) and fatty acid synthesis (FAS). We observed that acyl-CoA-DH expression was unaltered in the mutant mice, whereas FAS mRNA levels were decreased (Fig. 2 and quantification in supplemental Fig. 1B). T_3 treatment increased Acyl-CoA-DH transcripts to

Downloaded from https://academic.oup.com/endo/article/150/6/2940/2456385 by guest on 21 August 2022

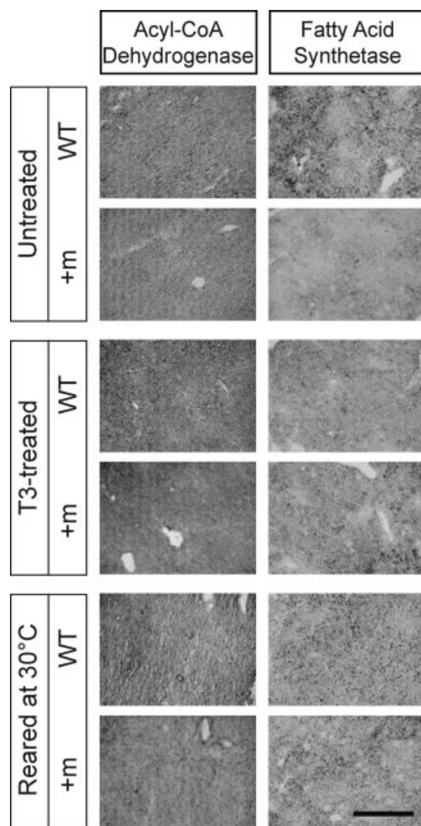

FIG. 2. *In situ* hybridization histochemistry on liver sections of untreated, T_3-treated, and 30 C acclimated wild-type (WT) mice and animals with a mutant TRα1 (+m), showing the mRNA expression of acyl-coenzyme A (Acyl-CoA) dehydrogenase and fatty acid synthetase. *Scale bar*, 500 μm.

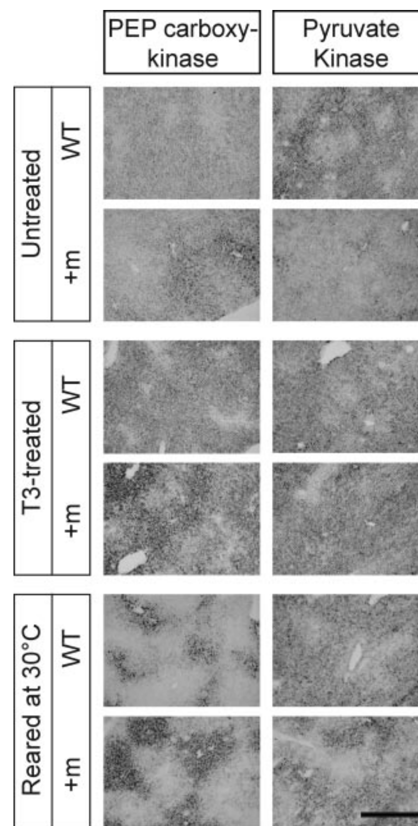

FIG. 3. *In situ* hybridization histochemistry on liver sections of untreated, T_3-treated, and 30 C acclimated wild-type (WT) mice and animals with a mutant TRα1 (+m), showing the mRNA expression of phosphoenolpyruvate (PEP) carboxykinase and PK. *Scale bar*, 500 μm.

some extent in both genotypes. Similar observations were obtained in mice reared at 30 C, where the hypermetabolic phenotype of the mutant mice is reversed. In contrast, the expression of FAS normalized to wild-type levels upon T_3 treatment and at thermoneutrality. These results suggest that the FAS expression is not affected by a mutant TRα1 acting in the liver but instead responds to the overall metabolic activity, which is high in the untreated mutants and ameliorated by either treatment (11).

We then analyzed glucose metabolism using *in situ* hybridization for key enzymes in gluconeogenesis (PEPCK) and glycolysis (PK). The expression of PEPCK mRNA was stronger in the mutant animals compared with wild-type controls, whereas the expression of PK mRNA was clearly reduced in the TRα1+m mice (Fig. 3 and supplemental Fig. 1B). To verify this, we also applied real-time PCR (qPCR), which showed a 2.4-fold increased PEPCK and a 2.2-fold reduced PK transcript levels in the TRα1+m animals (Fig. 4B, *top panels*).

Upon treatment with high doses of T_3, expression of PEPCK mRNA was induced in both genotypes, and a more zonated pattern was observed compared with the ubiquitous expression in the untreated animals. The corresponding qPCR analysis showed a 2-fold increase in PEPCK expression in the wild type upon T_3 treatment but only a slight nonsignificant increase in the mutant mice. That this increase is not as apparent as in the *in situ* hybridization might be due to the limited quantitative capacity of the *in situ* hybridization.

With regard to PK mRNA levels, T_3 treatment caused a decreased expression in the wild type but an increase in the mutants compared with untreated animals (Fig. 3 and supplemental Fig. 1B). Similar to PEPCK, the qPCR confirmed a 2-fold reduction in PK mRNA levels in T_3-treated wild types, whereas transcript levels were not significantly changed in the mutant animals (Fig. 4A, *top panels*).

When the mice were reared at thermoneutrality, an even more pronounced zonation of PEPCK and PK mRNA expression was observed by *in situ* hybridization (Fig. 3). Similar to room temperature, the *in situ* hybridization indicated higher PEPCK and lower PK expression in the mutants; however, this difference failed to reach significance when quantified by qPCR (Fig. 4D).

We then analyzed the mRNA expression of other genes involved in glucose handling using qPCR to identify additional effects of the mutant TRα1 on glucose metabolism. Transcript levels of lactate dehydrogenase and aldolase B showed no differences between the genotypes or upon T_3 treatment (Fig. 4A and statistics in supplemental Fig. 1A). Moreover, glucose-6-phosphatase mRNA levels were also not significantly different between the genotypes but decreased in both animal groups after T_3 treatment. Similarly, glucokinase was induced upon T_3 treatment as expected (22), but the expression levels did not differ between the genotypes. Thus, the mutant TRα1 had no strong effects on the expression of these genes, either under euthyroid or under hyperthyroid conditions.

Downloaded from https://academic.oup.com/endo/article/150/6/2940/2456385 by guest on 21 August 2022

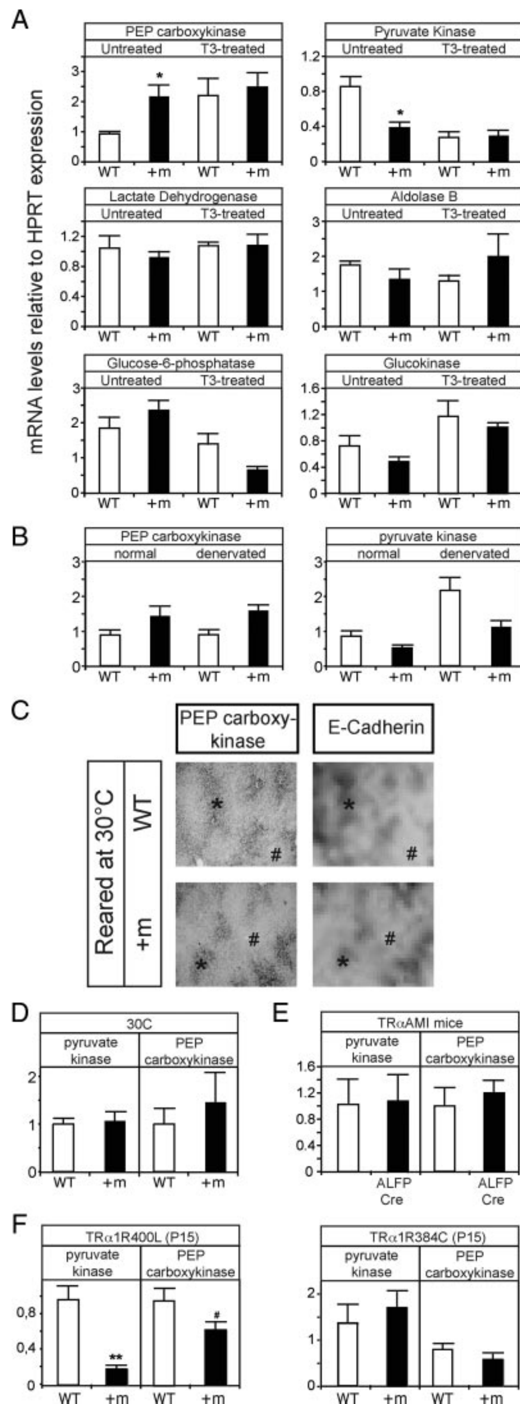

FIG. 4. A, mRNA levels of hepatic glucose metabolic genes in untreated and T_3-treated ($+T_3$) wild-type (WT) and mutant (+m) animals (*, $P < 0.05$ compared with untreated WT); B, mRNA levels of phosphoenolpyruvate (PEP) carboxykinase and PK in isolated liver slices of wild-type (WT) and mutant (+m) animals cultured for 6 h (to achieve denervation effects) in comparison with intact organs; C, colocalization of PEPCK and E-cadherin mRNA expression by double *in situ* hybridization histochemistry, showing regions expressing both (*) or neither (#) mRNA; D, quantification of PEPCK and PK mRNA levels in wild-type and TRα1+m mutants reared at 30 C using qPCR; E, hepatic mRNA expression of PK and PEPCK in TRαAMI mice, which liver-specifically express a mutant TRα1L400R upon Cre recombination (ALFP-Cre); F, mRNA levels of PK and PEPCK in P15 mice expressing either the mutant TRα1R384C or TRα1L400R (**, $P < 0.005$ compared with wild type; #, $P = 0.06$ compared with wild type).

To define the hepatic region in which the mutant TRα1 caused an up-regulated PEPCK mRNA expression, we applied double *in situ* hybridization histochemistry with probes for E-cadherin mRNA as periportal marker. The analysis revealed that the expression of PEPCK and E-cadherin mRNA overlapped in mice of both genotypes reared at 30 C (Fig. 4C). This demonstrates that PEPCK mRNA levels are up-regulated in the periportal areas of TRα1+m mutants.

Role of TRα1 in the regulation of hepatic PEPCK and PK

To investigate whether the changes in PEPCK and PK mRNA were caused by a direct hepatic action of the mutant TRα, slices of wild-type and mutant livers were cultured for 6 h, a time period long enough to mimic a denervated state, because the mRNA half-life of PEPCK and PK is around 90 min and effects mediated by changes in cAMP signaling manifest within 20 min (23, 24). Analysis by qPCR (Fig. 4B) revealed that the expression of PEPCK was unaffected as expected from the literature (25), whereas the expression of PK mRNA was more than 2-fold induced as a consequence of the denervation ($P < 0.05$). However, the differences between wild type and TRα1+m mutants persisted for both genes after denervation ($P < 0.05$), suggesting a direct hepatic effect of the mutant TRα1.

We then analyzed hepatic PEPCK and PK mRNA levels in mice, which upon Cre recombination express a mutant TRα1L400R receptor (15) specifically in hepatocytes (TRαAMI mice crossbred with ALFP-Cre mice). No difference was observed in the expression of the two genes in these animals (Fig. 4E), even upon propylthiouracil-induced hypothyroidism or after TH treatment (data not shown). To identify whether the absence of PEPCK and PK regulation in these animals might be caused by the different location of the TRα1 mutation (TRα1R384C *vs.* TRα1L400R), we analyzed the expression of these genes in postnatal d 15 (P15) TRαAMI mice, which express the mutant TRα1L400R in all tissues (Fig. 4F). In contrast to P15 TRα1R384C mice, where PEPCK and PK transcript levels were not different from littermate controls, the TRα1L400R mutants exhibited reduced PK and PEPCK transcript levels, indicating that the two mutations differ in their consequences for hepatic metabolism.

Physiological consequences in TRα1+m mice

Because many rate-limiting enzymes are posttranscriptionally modified, we determined the enzymatic activities of PEPCK and PK in liver homogenates to corroborate the quantitative data obtained by qPCR. Our results showed a shift from glycolysis to gluconeogenesis in TRα1+m mice (Fig. 5A), a situation comparable to the one found in fasted wild-type mice. However, this ratio was not further altered in the mutants after 24 h fasting. Similar results were obtained by treatment with T_3 and by rearing at thermoneutrality; both conditions increased glucose production over glucose consumption in the wild-type animals but had no effect on the mutant mice.

We then determined the hepatic glycogen content in the liver of these animals. The results showed completely depleted glycogen stores in TRα1+m mice, again comparable to the situation found in fasted animals (Fig. 5B). Although T_3 treatment de-

Downloaded from https://academic.oup.com/endo/article/150/6/2940/2456385 by guest on 21 August 2022

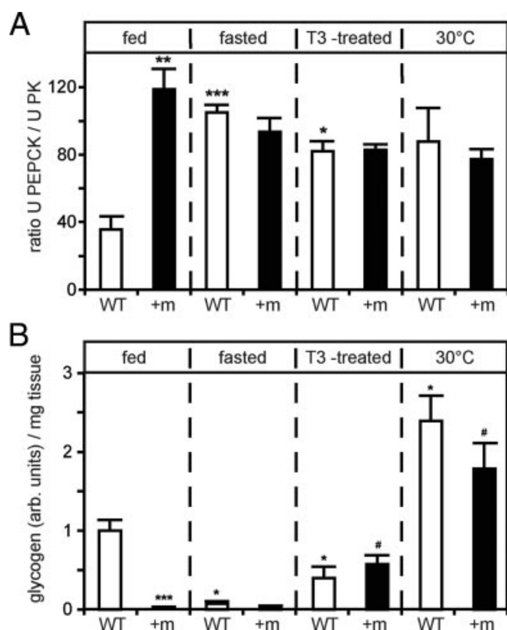

FIG. 5. Ratio between the enzymatic activities in Units (U) of PEPCK and PK (A) and hepatic glycogen content (B) in untreated, 24-h fasted (fast), T_3-treated ($+T_3$) wild-type (WT), and TRα1+m (+m) mice and animals that were reared at thermoneutrality (30 C). *, $P < 0.05$ compared with untreated WT; **, $P < 0.005$ compared with untreated WT; ***, $P < 0.001$ compared with untreated WT; #, $P < 0.05$ compared with untreated TRα1+m; arb., Arbitrary.

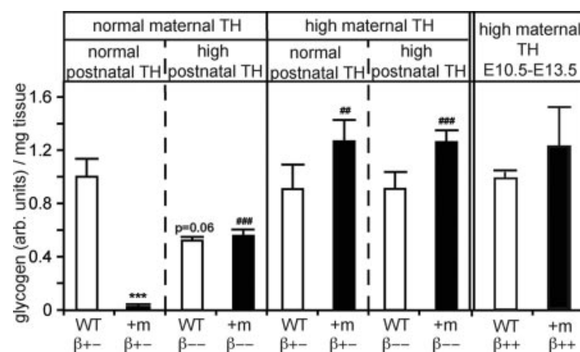

FIG. 6. Hepatic glycogen content in wild-type (WT) and TRα1+m mice (+m), wild-type and TRα1+m mice that were born from dams with high maternal TH, wild-type and TRα1+m animals that have been exposed to high levels of TH postnatally by the inactivation of TRβ (β−−), combinations of the latter two treatments and wild-type and TRα1+m mice born from dams that were exposed orally to high levels of T_3 during E10.5–E13.5 of the pregnancy. ***, $P < 0.001$ compared with untreated WT; ##, $P < 0.005$ compared with untreated TRα1+m; ###, $P < 0.001$ compared with untreated TRα1+m; arb., Arbitrary.

creased the glycogen content in wild-type mice by half, mutant mice increased their hepatic glycogen content to T_3-treated wild-type levels. At thermoneutrality, both genotypes exhibited elevated glycogen levels that were significantly higher than in untreated wild-type mice.

Despite depleted glycogen, the mutant mice handled a prolonged fasting (24 h) as efficiently as wild-type mice (glucose levels fed wild type 7.28 ± 0.30 *vs.* TRα1+m 8.2 ± 0.13; fasted wild type 5.74 ± 0.32 *vs.* TRα1+m 5.42 ± 0.28 mmol/liter). We observed neither upon T_3 treatment nor at thermoneutrality a significant difference in blood glucose levels between the genotypes (T_3-treated, wild type 7.28 ± 0.39 *vs.* TRα1+m 6.36 ± 0.27; 30 C acclimation, wild type 7.24 ± 0.53 *vs.* TRα1+m 8.5 ± 0.35 mmol/liter).

To determine the developmental window at which the deranged setting of glycogen metabolism occurred, we reactivated the mutant receptor in TRα1+m mice at different time periods of development and analyzed the glycogen content in the adult animal. To reactivate the mutant TRα1 postnatally, we crossed TRα1+m animals with hyperthyroid $TR\beta^{--}$ mice, thus obtaining TRα1+m $TR\beta^{--}$ double mutants, which exhibit 10-fold elevated TH levels from birth onward (5). These animals exhibited partial restoration of glycogen stores, whereas hyperthyroid $TR\beta^{--}$ controls had a 50% decreased glycogen content (Fig. 6).

Then we reactivated the mutant receptor during fetal development using the hyperthyroid $TR\beta^{--}$ dams. These dams expose the TRα1+m embryos to high levels of TH throughout gestation, thus restoring TRα1 signaling *in utero* (5). Strikingly, the high levels of maternal TH during embryogenesis normalized the glycogen deficiency in adult TRα1+m mice. Furthermore, the glycogen content was also restored in $TR\beta^{--}$ and TRα1+m $TR\beta^{--}$ double-mutant animals. To avoid potential effects of the maternal TRβ inactivation, we also treated pregnant dams orally with T_3 from embryonic d 10.5 (E10.5) until E13.5. Also, this treatment restored the glycogen deficiency in the adult offspring mice, indicating that the TRα1 aporeceptor affects the metabolic setpoint in the offspring during this developmental windows.

Discussion

Effects of TH on hepatic glucose metabolism

The livers of TRα1+m mice are affected by two factors: an impaired hepatic TRα1 signaling and a centrally induced hypermetabolism. Our analysis revealed that the mutant animals exhibited depleted glycogen stores despite increased gluconeogenesis and decreased glycolysis. This phenotype was mainly caused by the hypermetabolic state of the animals, only a slight difference in the mRNA expression of the rate-limiting gene PEPCK remained at thermoneutrality, when the metabolism was normalized.

Because the TRα1+m animals represent a receptor-mediated hypothyroidism, an increased hepatic glucose production is unexpected. Hypothyroidism is associated with decreased gluconeogenesis (25, 26), whereas hyperthyroidism causes increased PEPCK expression and decreased PK mRNA (27), as also found in our T_3-treated wild-type mice.

Given the prominent role of TRα1 in the brain, a central effect could be inferred, because alterations in the hypothalamus-liver circuit can contribute to hyperglycemia through the elevation of gluconeogenesis, *e.g.* in diabetes (28). Moreover, electrical stimulation of the sympathetic nervous system via the ventromedial hypothalamus is known to increase PEPCK activity and suppress PK (29) while emptying glycogen stores (30). Accordingly, when livers of wild-type and mutant animals were cultured as denervated slices for 6 h, PK mRNA was 2-fold induced in both genotypes, probably as a consequence of an abolished central inhibition. However, neither PK nor PEPCK mRNA expression normalized in the mutant explant tissues. This correlates with

Downloaded from https://academic.oup.com/endo/article/150/6/2940/2456385 by guest on 21 August 2022

studies on surgically denervated rat livers, which suggested that any central contributions on PEPCK mRNA regulation are negligible under eu- and hyperthyroid conditions (25).

A direct hepatic effect of the mutant TRα1 is supported by the observation that the stimulation of PEPCK mRNA occurred specifically in the periportal zone, where gluconeogenesis is higher than around the central veins (31) and where TRα1 is the only expressed TR isoform (32, 33).

In contrast, mutant mice expressing the TRα1L400R mutation exclusively in the liver did not show any abnormalities in PEPCK and PK mRNA expression; however, animals expressing TRα1L400R in all tissues showed a different expression of PEPCK and PK than TRα1R384C mice. The different consequences of the two mutations for hepatic metabolism are most likely caused by their location, which may affect the interactions of the receptors with nuclear cofactors (34). Therefore, the absence of a hepatic phenotype in liver-specific TRα1R400L animals does not exclude a liver-specific action of TRα1R384C. However, a possible transcriptional effect of a mutant TRα1R384C on PEPCK or PK seems of minor physiological relevance, regarding the fact that the ratio of enzymatic activity between PEPCK and PK normalized in the mutant animals at thermoneutrality.

Consequences for glycogen storage

Together with the enzymatic activities of PEPCK and PK, the glycogen content of the liver is a valuable metabolic readout for hepatic glucose flux. In wild-type mice, T_3 treatment up-regulated gluconeogenesis but decreased glycogen content by half, reflecting an increased systemic glucose demand. The situation in the mutant mice with low glycogen despite high gluconeogenesis is remarkable, because glucose produced from gluconeogenesis is usually exclusively used to fuel the glycogen production, a condition termed the glucose paradox (35, 36). This paradox could be observed in animals of both genotypes reared at thermoneutrality, where increased PEPCK and suppressed PK lead to large amounts of stored glycogen. In the mutant animals reared at room temperature, glucose was not stored as glycogen but exported into the bloodstream. However, it cannot be excluded that there is a constant flux in and out of glycogen as suggested by the glucose paradox (35) because only steady-state levels of glycogen have been determined.

TRα1+m mice are in a chronically fasted state

The physiological condition of increased gluconeogenesis over glycolysis and depleted glycogen stores indicated that TRα1+m mice were in a chronically fasted state, comparable to the situation found in wild-type mice after 24 h food deprivation (27). In fasting wild-type mice, the hepatic glycogen stores were rapidly mobilized to maintain euglycemia; however, glycogenolysis accounts for only 50% of the glucose demand in the first 24 h fasting, whereas the remaining half is covered by gluconeogenesis (37). It was thus not surprising that increased gluconeogenesis in the mutant animals was also sufficient to meet the glucose demand built up by the 24-h fast. It remains, however, uncertain whether this system is flexible enough to cope with longer starvation periods or an immediate glucose demand by, for example, insulin stimulation.

The chronically fasted state of TRα1+m mice partially reflected the situation found in human metabolic disorders such as cancer cachexia (38) or glycogen storage disease type 0, a condition in which a defective glycogen synthetase prevents accumulation of glycogen (39). Thus, TRα1+m mice provide a valuable animal model to identify therapeutic approaches enhancing the treatment of similar metabolic disorders using TRα1 specific pathways.

The glycogen deficiency is programmed during embryonal development

The observation that the hypermetabolic phenotype can be reversed at thermoneutrality, which functionally deinnervates the BAT, strongly suggests a central origin of the dysregulations caused by the mutant TRα1 (11). Because the glycogen deficiency was normalized in TRα1+m mice at thermoneutrality and when the animals were exposed to high levels of maternal TH during pregnancy, the developmental defect seemed to be caused by the aporeceptor state of TRα1 in early brain development. Moreover, the 50% reduction of hepatic glycogen content observed in $TR\beta^{--}$ mice was also restored by exposure to high TH levels during fetal development. However, because T_4 serum levels are somewhat lower in $TR\beta^{--}$ mice born by dams with high levels of TH compared with $TR\beta^{--}$ animals from euthyroid dams (5), different mechanisms from those in TRα1+m mice could contribute to this effect.

That the glycogen deficiency is restored by embryonal reactivation of the mutant receptor was not surprising, because it is well known that impaired TRα1 signaling during pregnancy causes suboptimal neuronal development, a situation also occurring during maternal hypothyroxinemia (40). This condition can lead to various irreversible central nervous system disturbances (41), different setpoints of endocrine circuits such as the hypothalamic-pituitary-thyroid axis (42) and an impaired development of several tissues such as the heart and the lungs (43). All these deficiencies persist into adulthood and occur even if the maternal hypothyroxinemia was only mild or moderate (40). Because insulin sensitivity is negatively associated with TH status in intrauterine retarded newborns (44), it was not surprising that impaired TRα1 signaling during pregnancy also affected the metabolic setpoint of the offspring.

In summary, our results demonstrate that impairments in TH metabolism during embryonic development can cause metabolic aberrations in the offspring. These findings add another aspect to the growing evidence that proper maternal TH supply is of considerable importance for the well-being of the child and underline the necessity for adequate control of TH levels during pregnancy.

Acknowledgments

We are grateful to Dr. Anneke Alkemade and Dr. Maria Sjögren for their contributions, Karin Wallis for critically reading the manuscript, Ellen Kaptein for technical assistance, Dr. Björn Rozell for excellent technical expertise, and Prof. Karl Bauer for the plasmid containing the probe for deiodinase type I. We also want to thank Prof. Marc Gilbert and Dr.

Downloaded from https://academic.oup.com/endo/article/150/6/2940/2456385 by guest on 21 August 2022

Marie Björnholm for fruitful discussions. Furthermore, J.M. thanks the EMBO and the Deutsche Forschungsgemeinschaft for financial support, and B.V. is grateful for financial support from the Swedish Cancer Society and the Swedish Science Council.

Address all correspondence and requests for reprints to: Dr. Jens Mittag, Karolinska Institutet, Department of Cell and Molecular Biology, von Eulers väg 3, 17177 Stockholm, Sweden. E-mail: jens.mittag@ki.se.

The work of K.G. and F.F. is supported by the Agence Nationale pour la Recherche (Signator contract), the CASCADE (Chemicals as contaminants in the food chain: a Network of Excellence for research, risk assessment, and education) European network of excellence (FOOD-CT-2004-506319), and the CRESCENDO (Consortium for Research into Nuclear Receptors in Development and Aging) European integrated project (LSHM-CT-2005-018652).

Disclosure Summary: The authors have nothing to disclose.

References

1. **Kim B** 2008 Thyroid hormone as a determinant of energy expenditure and the basal metabolic rate. Thyroid 18:141–144
2. **Lazar MA** 1993 Thyroid hormone receptors: multiple forms, multiple possibilities. Endocr Rev 14:184–193
3. **Bernal J, Guadaño-Ferraz A, Morte B** 2003 Perspectives in the study of thyroid hormone action on brain development and function. Thyroid 13:1005–1012
4. **Guadaño-Ferraz A, Benavides-Piccione R, Venero C, Lancha C, Vennström B, Sandi C, DeFelipe J, Bernal J** 2003 Lack of thyroid hormone receptor α1 is associated with selective alterations in behavior and hippocampal circuits. Mol Psychiatry 8:30–38
5. **Wallis K, Sjögren M, van Hogerlinden M, Silberberg G, Fisahn A, Nordström K, Larsson L, Westerblad H, Morreale de Escobar G, Shupliakov O, Vennström B** 2008 Locomotor deficiencies and aberrant development of subtype-specific GABAergic interneurons caused by an unliganded thyroid hormone receptor α1. J Neurosci 28:1904–1915
6. **Gullberg H, Rudling M, Saltó C, Forrest D, Angelin B, Vennström B** 2002 Requirement for thyroid hormone receptor β in T_3 regulation of cholesterol metabolism in mice. Mol Endocrinol 16:1767–1777
7. **Weiss RE, Murata Y, Cua K, Hayashi Y, Seo H, Refetoff S** 1998 Thyroid hormone action on liver, heart, and energy expenditure in thyroid hormone receptor β-deficient mice. Endocrinology 139:4945–4952
8. **Refetoff S, Weiss RE, Usala SJ** 1993 The syndromes of resistance to thyroid hormone. Endocr Rev 14:348–399
9. **Tinnikov A, Nordström K, Thorén P, Kindblom JM, Malin S, Rozell B, Adams M, Rajanayagam O, Pettersson S, Ohlsson C, Chatterjee K, Vennstrom B** 2002 Retardation of post-natal development caused by a negatively acting thyroid hormone receptor α1. EMBO J 21:5079–5087
10. **Venero C, Guadaño-Ferraz A, Herrero AI, Nordström K, Manzano J, de Escobar GM, Bernal J, Vennström B** 2005 Anxiety, memory impairment, and locomotor dysfunction caused by a mutant thyroid hormone receptor α1 can be ameliorated by T_3 treatment. Genes Dev 19:2152–2163
11. **Sjögren M, Alkemade A, Mittag J, Nordström K, Katz A, Rozell B, Westerblad H, Arner A, Vennström B** 2007 Hypermetabolism in mice caused by the central action of an unliganded thyroid hormone receptor α1. EMBO J 26:4535–4545
12. **Höppner W, Seitz HJ** 1989 Effect of thyroid hormones on glucokinase gene transcription in rat liver. J Biol Chem 264:20643–20647
13. **Flores-Morales A, Gullberg H, Fernandez L, Ståhlberg N, Lee NH, Vennström B, Norstedt G** 2002 Patterns of liver gene expression governed by TRβ. Mol Endocrinol 16:1257–1268
14. **Parviz F, Matullo C, Garrison WD, Savatski L, Adamson JW, Ning G, Kaestner KH, Rossi JM, Zaret KS, Duncan SA** 2003 Hepatocyte nuclear factor 4α controls the development of a hepatic epithelium and liver morphogenesis. Nat Genet 34:292–296
15. **Quignodon L, Vincent S, Winter H, Samarut J, Flamant F** 2007 A point mutation in the activation function 2 domain of thyroid hormone receptor α1 expressed after CRE-mediated recombination partially recapitulates hypothyroidism. Mol Endocrinol 21:2350–2360
16. **Schäfer M, Day R** 1995 In situ hybridization techniques to study processing enzyme expression at the cellular level. J Neurosci Methods 23:16–44
17. **Friesema EC, Kuiper GG, Jansen J, Visser TJ, Kester MH** 2006 Thyroid hormone transport by the human monocarboxylate transporter 8 and its rate-limiting role in intracellular metabolism. Mol Endocrinol 20:2761–2772
18. **Van Der Vies J** 1954 Two methods for the determination of glycogen in liver. Biochemical J 57:410–416
19. **Thompson MD, Monga SP** 2007 WNT/β-catenin signaling in liver health and disease. Hepatology 45:1298–1305
20. **Plateroti M, Kress E, Mori JI, Samarut J** 2006 Thyroid hormone receptor α1 directly controls transcription of the β-catenin gene in intestinal epithelial cells. Mol Cell Biol 26:3204–3214
21. **Heuer H, Maier MK, Iden S, Mittag J, Friesema EC, Visser TJ, Bauer K** 2005 The monocarboxylate transporter 8 linked to human psychomotor retardation is highly expressed in thyroid hormone-sensitive neuron populations. Endocrinology 146:1701–1706
22. **Narkewicz MR, Iynedjian PB, Ferre P, Girard J** 1990 Insulin and tri-iodothyronine induce glucokinase mRNA in primary cultures of neonatal rat hepatocytes. Biochem J 271:585–589
23. **Chen G** 2007 Liver lipid molecules induce PEPCK-C gene transcription and attenuate insulin action. Biochem Biophys Res Commun 361:805–810
24. **Hanson RW, Reshef L** 1997 Regulation of phosphoenolpyruvate carboxykinase (GTP) gene expression. Annu Rev Biochem 66:581–611
25. **Klieverik LP, Sauerwein HP, Ackermans MT, Boelen A, Kalsbeek A, Fliers E** 2008 Effects of thyrotoxicosis and selective hepatic autonomic denervation on hepatic glucose metabolism in rats. Am J Physiol 294:E513–E520
26. **Chidakel A, Mentuccia D, Celi FS** 2005 Peripheral metabolism of thyroid hormone and glucose homeostasis. Thyroid 15:899–903
27. **Pilkis SJ, Granner DK** 1992 Molecular physiology of the regulation of hepatic gluconeogenesis and glycolysis. Annu Rev Physiol 54:885–909
28. **Pocai A, Lam TK, Gutierrez-Juarez R, Obici S, Schwartz GJ, Bryan J, Aguilar-Bryan L, Rossetti L** 2005 Hypothalamic K_AT_P channels control hepatic glucose production. Nature 434:1026–1031
29. **Shimazu T, Ogasawara S** 1975 Effects of hypothalamic stimulation on gluconeogenesis and glycolysis in rat liver. Am J Physiol 228:1787–1793
30. **Puschel GP** 2004 Control of hepatocyte metabolism by sympathetic and parasympathetic hepatic nerves. Anat Rec 280:854–867
31. **Chen KS, Katz J** 1988 Zonation of glycogen and glucose syntheses, but not glycolysis, in rat liver. Biochem J 255:99–104
32. **Zandieh Doulabi B, Platvoet-ter Schiphorst M, van Beeren HC, Labruyere WT, Lamers WH, Fliers E, Bakker O, Wiersinga WM** 2002 TRβ1 protein is preferentially expressed in the pericentral zone of rat liver and exhibits marked diurnal variation. Endocrinology 143:979–984
33. **Zandieh-Doulabi B, Platvoet-ter Schiphorst M, Kalsbeek A, Wiersinga WM, Bakker O** 2004 Hyper and hypothyroidism change the expression and diurnal variation of thyroid hormone receptor isoforms in rat liver without major changes in their zonal distribution. Mol Cell Endocrinol 219:69–75
34. **Liu YY, Heymann RS, Moatamed F, Schultz JJ, Sobel D, Brent GA** 2007 A mutant thyroid hormone receptor α antagonizes peroxisome proliferator-activated receptor α signaling in vivo and impairs fatty acid oxidation. Endocrinology 148:1206–1217
35. **Youn JH, Bergman RN** 1990 Enhancement of hepatic glycogen by gluconeogenic precursors: substrate flux or metabolic control? Am J Physiol 258:E899–E906
36. **Katz J, McGarry JD** 1984 The glucose paradox. Is glucose a substrate for liver metabolism? J Clin Invest 74:1901–1909
37. **Savage DB, Petersen KF, Shulman GI** 2007 Disordered lipid metabolism and the pathogenesis of insulin resistance. Physiol Rev 87:507–520
38. **Esper DH, Harb WA** 2005 The cancer cachexia syndrome: a review of metabolic and clinical manifestations. Nutr Clin Pract 20:369–376
39. **Orho M, Bosshard NU, Buist NR, Gitzelmann R, Aynsley-Green A, Blümel P, Gannon MC, Nuttall FQ, Groop LC** 1998 Mutations in the liver glycogen synthase gene in children with hypoglycemia due to glycogen storage disease type 0. J Clin Invest 102:507–515
40. **Morreale de Escobar G, Obregón MJ, del Rey FE** 2007 Iodine deficiency and brain development in the first half of pregnancy. Public Health Nutr 10:1554–1570
41. **Zoeller RT, Rovet J** 2004 Timing of thyroid hormone action in the developing brain: clinical observations and experimental findings. J Neuroendocrinol 16:809–818
42. **Alonso M, Goodwin C, Liao X, Page D, Refetoff S, Weiss RE** 2007 Effects of maternal levels of thyroid hormone (TH) on the hypothalamus-pituitary-thyroid set point: studies in TH receptor β knockout mice. Endocrinology 148:5305–5312
43. **van Tuyl M, Blommaart PE, de Boer PA, Wert SE, Ruijter JM, Islam S, Schnitzer J, Ellison AR, Tibboel D, Moorman AF, Lamers WH** 2004 Prenatal exposure to thyroid hormone is necessary for normal postnatal development of murine heart and lungs. Dev Biol 272:104–117
44. **Setia S, Sridhar MG, Koner BC, Bobby Z, Bhat V, Chaturvedula L** 2007 Increased insulin sensitivity in intrauterine growth retarded newborns: do thyroid hormones play a role? Clin Chim Acta 376:37–40

Downloaded from https://academic.oup.com/endo/article/150/6/2940/2456385 by guest on 21 August 2022